Sign-Reversing Hall Effect in Atomically Thin High-Temperature $Bi_{2.1}Sr_{1.9}CaCu_{2.0}O_{8+\delta}$ Superconductors

S. Y. Frank Zhao,[1] Nicola Poccia,[1] Margaret G. Panetta,[1] Cyndia Yu,[1] Jedediah W. Johnson,[1] Hyobin Yoo,[1] Ruidan Zhong,[2] G. D. Gu,[2] Kenji Watanabe,[3] Takashi Taniguchi,[3] Svetlana V. Postolova,[4,5] Valerii M. Vinokur,[6,7] and Philip Kim[1,*]

[1]*Department of Physics, Harvard University, Cambridge, Massachusetts 02138, USA*
[2]*Department of Condensed Matter Physics and Materials Science, Brookhaven National Laboratory, Upton, New York 11973, USA*
[3]*National Institute for Materials Science, Namiki 1-1, Tsukuba, Ibaraki 305-0044, Japan*
[4]*Institute for Physics of Microstructures RAS, Nizhny Novgorod 603950, Russia*
[5]*Rzhanov Institute of Semiconductor Physics SB RAS, Novosibirsk 630090, Russia*
[6]*Materials Science Division, Argonne National Laboratory, Argonne, Illinois 60439, USA*
[7]*Consortium for Advanced Science and Engineering, Office of Research and National Laboratories, University of Chicago, Chicago, Illinois 60637, USA*

(Received 20 September 2018; revised manuscript received 31 January 2019; published 20 June 2019)

We developed novel techniques to fabricate atomically thin $Bi_{2.1}Sr_{1.9}CaCu_{2.0}O_{8+\delta}$ van der Waals heterostructures down to two unit cells while maintaining a transition temperature T_c close to the bulk, and carry out magnetotransport measurements on these van der Waals devices. We find a double sign change of the Hall resistance R_{xy} as in the bulk system, spanning both below and above T_c. Further, we observe a drastic enlargement of the region of sign reversal in the temperature-magnetic field phase diagram with decreasing thickness of the device. We obtain quantitative agreement between experimental $R_{xy}(T, B)$ and the predictions of the vortex dynamics-based description of Hall effect in high-temperature superconductors both above and below T_c.

DOI: 10.1103/PhysRevLett.122.247001

Tunable van der Waals (vdW) structures based on atomically thin superconducting $Bi_{2.1}Sr_{1.9}CaCu_{2.0}O_{8+\delta}$ (BSCCO) crystals enable exploring unconventional electronic properties of high-temperature superconductors (HTS) [1]. One of the most insightful tools to study properties of electronic systems is the Hall effect. However, the behavior of Hall resistance in HTS, in particular its sign change, remains poorly understood. As temperature T decreases through the fluctuation region approaching the transition temperature T_c, the Hall resistance decreases and changes its sign relative to that of the normal state. Then $R_{xy}(T)$ reverses sign again before vanishing at low temperatures [2,3].

A rich theoretical lore attributes the Hall anomalies to either vortex pinning [4], details of the vortex core electronic spectrum [5,6], hydrodynamic effects [7], superconducting fluctuations [8–10], Berry phase [11], and charges in the vortex core [12]. However, neither the explanation nor the consensus of the Hall behavior in the entire temperature range was achieved. A comprehensive explanation of the Hall sign reversal appeared in [13], which completely took into account both topological and normal excitation scattering effects, and especially the fact that the density of normal excitations at the vortex core differs from that far from the vortex. The results of [13] established that the sign-reversed Hall effect occurs in the temperature range where contribution from the vortex motion dominates over the effects from normal excitations and is controlled by the excess charge at the vortex core and the magnitude of the parameter $\Delta\tau/\hbar$, where $\Delta(T)$ is the superconducting gap and τ is the scattering time of normal quasiparticles.

In this Letter, we report the fabrication of superconducting (SC) atomically thin BSCCO crystals with strongly enhanced fluctuation effects and their magnetotransport properties. We observe Hall sign reversal which smoothly spans the superconducting transition, and persists both deep into the superconducting state and 5 K above T_c. We present a quantitative description of the observed phase boundary separating the normal and sign-reversed Hall domains [13] in terms of vortex dynamics in the entire temperature interval both below and above T_c, revealing a deep connection between vortexlike excitations above T_c [14,15] and superconducting fluctuations.

We prepare our few unit-cell (UC) thick BSCCO by mechanically exfoliating optimally doped $Bi_{2.1}Sr_{1.9}CaCu_{2.0}O_{8+\delta}$ in an argon filled glovebox. After conventional nanofabrication steps, BSCCO typically becomes insulating [16] due to chemical degradation [17] and oxygen escape [18]. We have developed a high-resolution stencil mask technique (see Supplemental Material [19]), allowing us to fabricate samples entirely in an argon environment without exposure to heat or chemicals, and subsequently sealed with a top hexagonal boron nitride (h-BN) layer. Figures 1(a) and 1(b) show our typical Hall bar and a cross-sectional scanning TEM image of our vdW heterostructure, where dark spots

 © 2019 American Physical Society

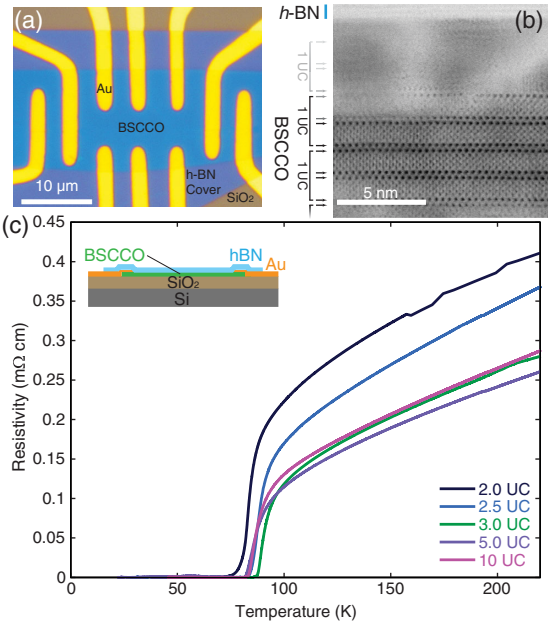

FIG. 1. van der Waals BSCCO device. (a) Optical image of Hall bar device, showing BSCCO with contacts and hexagonal boron nitride (h-BN) cover, as drawn in the inset below. (b) Cross-sectional view of a typical device in scanning TEM. Columns of atoms are visible as dark spots. Black arrows point to the location of bismuth oxide layers (darkest spots), while gray arrows show their extrapolated positions. (c) Resistivity as a function of temperature for vdW devices of a different thickness.

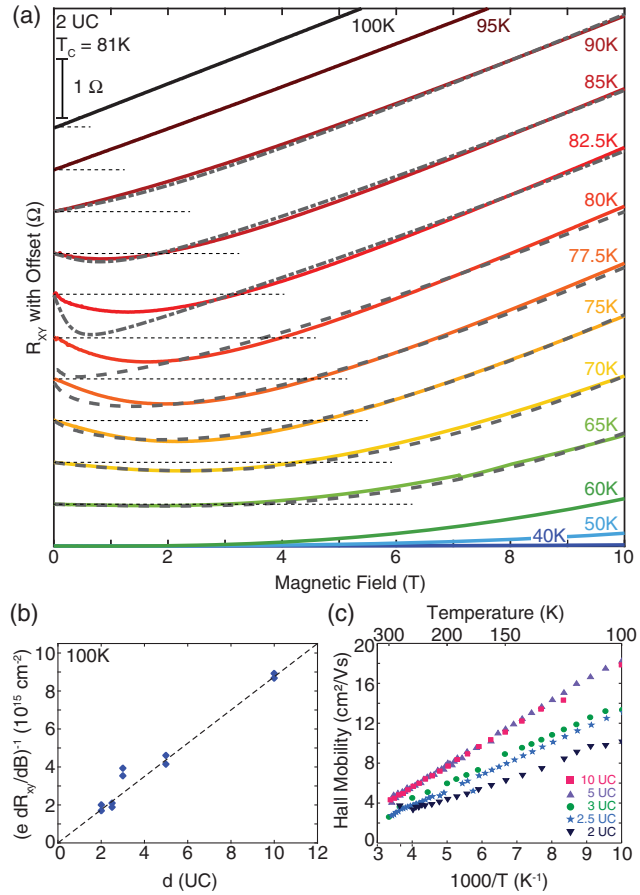

FIG. 2. Hall effect measurements. (a) Hall resistance for a 2 UC sample. The curves are vertically shifted for clarity, the horizontal dashed lines mark $R_{xy} = 0$. Below 60 K, the Hall effect has the same sign as in the normal state. Above 60 K the sign reversal appears at magnetic fields $B < 5$ T. Dashed and dash-dotted lines show fits to the data (solid lines). (b) Inverse Hall resistance increases linearly with sample thickness in our devices, demonstrating good oxygen dopant retention down to 2 UCs. Data taken at 100 K. (c) Device mobility increases as samples become thicker, eventually saturating at 5 UC.

are individual columns of atoms. The darkest of these are bismuth (arrows). While the outermost layers of BSCCO became amorphous, inner layers are left pristine, and retain T_c close to the bulk value. The amorphous outer layers are likely the result of water vapor traces leaking through the h-BN/SiO_2 interface, and this constrains us to devices above 2 UC.

Figure 1(c) shows the resistivity ρ as a function of temperature T for BSCCO devices between 2 and 10 UC. We find that at a given temperature T, resistivity ρ increases as the thickness of the sample d decreases. We have normalized our resistance data with the atomic force microscopy thickness, which is sensitive to the highly resistive amorphous surface layer. The $\rho(T)$ dependence is linear in the normal region, consistent with BSCCO near optimal doping [30] and exhibits a SC transition, at temperature slightly lower than the bulk one [31].

To describe the SC transition in $\rho(T)$ and determine the transition temperature T_c, we employ the framework of superconducting fluctuations (SF) [32–34], accounting for all fundamental SF contributions to conductivity: Aslamazov-Larkin, the SF change in the density of states of normal excitations, and the dominant Maki-Thompson contribution [34,35], using both T_c and the pair-breaking parameter $\delta = h/16k_BT\tau_\phi$ as fitting parameters. The phase-breaking time is assumed to be $\tau_\phi \sim T^{-1}$ [36]; see details in Supplemental Material [19]. For all samples, the extracted T_c (given in Supplemental Material [19]) is very close to the temperature of the inflection point, i.e., the temperature where dR/dT is maximal [35,37], and lies at the foot of $\rho(T)$. As a consistency check, numerous comparative studies [38,39] of bulk HTS demonstrated that T_c extracted from magnetic susceptibility agrees with the T_c from the inflection point.

Figure 2(a) presents the Hall data for a 2 UC device (solid lines), and, as usual, the odd component of $R_{xy}(B)$ is shown in order to eliminate effects from device geometric imperfections. In the normal state far above T_c ($T \geq 100$ K), the Hall resistance R_{xy} is linear in applied magnetic field B. Figure 2(b) shows the quantity $(edR_{xy}/dB)^{-1}$ measured at 100 K, which scales linearly with d, implying an excellent oxygen dopant retention in each CuO_2 plane, despite the

fact that mobile oxygen dopants [18] escape from our crystals over time. The 3 UC sample, the only device fabricated and cooled down in the same day, contains a higher carrier density, which agrees with the slightly increased T_c [Fig. 1(c)].

The Hall mobility $\mu_H = R_{xy}d/B\rho_{xx}$ is shown in Fig. 2(c). Below 5 UC, μ_H decreases with d, due to the increasing ratio of highly resistive (yet noninsulating) surface layers compared to pristine interior layers [see Fig. 1(b)], both of which contribute to the Hall and resistivity measurements in parallel. All our samples exhibit the trend $\mu_H \sim T^{-1}$ for $T \gg T_c$, suggesting that the normal carrier momentum relaxation time is $\tau_p \sim T^{-1}$ regardless of d.

Approaching T_c, $R_{xy}(B)$ becomes nonlinear [Fig. 2(a)]. The first sign reversal is observed about 5 K above T_c, up to 95 K for our most highly doped sample [Fig. 2(a) and Supplemental Material [19]]. The dip in $R_{xy}(B)$ becomes increasingly pronounced as temperature decreases and the region of negative sign extends from zero field to $B = 4.7$ T at about $T = 75$ K. Upon further cooling, $R_{xy}(B)$ flattens again and the B interval of the negative R_{xy} shrinks, until completely vanishing at $T \approx 60$ K (see also Sec. F in the Supplemental Material [19]). Then $R_{xy}(B)$ remains positive at all fields, until it disappears into the noise at $T \approx 40$ K.

The temperature evolution of $R_{xy}(T)$ at fixed B [Fig. 3(a)] highlights a double sign-reversal temperature interval. Figure 3(b) summarizes regions of sign reversal for the samples with similar doping and different thickness d. The $R_{xy}(T, B) < 0$ domain grows with decreasing d, while extending across and above T_c in all our samples.

The Hall sign reversal in high T_c is usually well pronounced in the mixed state below T_c extracted from the SF framework, the temperature where Cooper pair lifetime becomes infinite [30,40]. In conventional superconductors, Hall sign reversal usually occurs in the Gaussian fluctuations regime at $T > T_c$ [41,42]. However, there are experiments hinting at Hall sign reversal occurring slightly above T_c in 100–400 nm thick cuprate films [43,44]. In our atomically thin BSCCO flakes, the Hall sign-reversal region persists well above T_c (by 5 K). Importantly, in our 3 UC device with the highest T_c, sign reversal persists up to $4.1T$ at the onset $T_c \approx 90$ K of our bulk crystal [31], and up to $T_{\mathrm{HSR}} \approx 95$ K (see Supplemental Material [19], Sec. C), i.e., a few kelvins above the highest T_c for the bulk Bi-2212 family.

That Hall resistance $R_{xy}(T)$ does not exhibit any drastic changes when crossing T_c (Fig. 3) suggests the possibility of a unique universal description of the Hall effect over the entire experimental range of temperatures and magnetic fields. Such a universal description is provided by the time-dependent Ginzburg-Landau (TDGL) equation [3]. In the fluctuation regime at $T \gtrsim T_c$, where fluctuational order parameter is small, TDGL can be linearized. In this Gaussian approximation, the Hall resistance can be calculated with [10] accounting for SF effects. At $T < T_c$ the electromagnetic response of superconductors is governed by vortex dynamics. In this regime, the Ginzburg-Landau

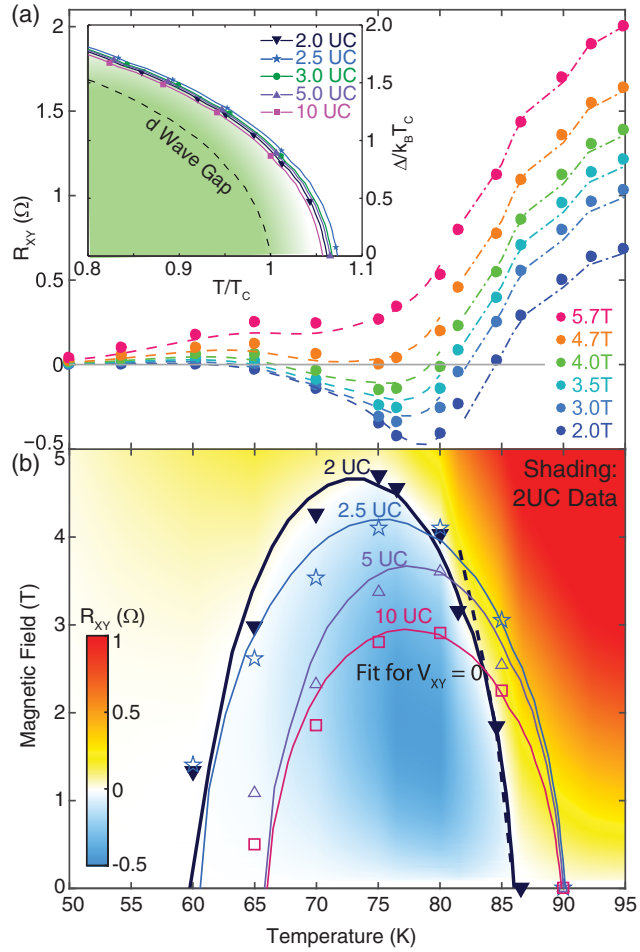

FIG. 3. The double sign change. (a) Temperature dependencies $R_{xy}(T)$ at fixed magnetic fields for the 2 UC device. Fits above (dash-dotted) and below (dashed lines) T_c are superimposed on experimental data (symbols). Inset: Superconducting gap extracted from fits for all samples using Eq. (1). T_c is the temperature extracted from the analysis of $R_{xx}(T)$ in the framework of superconducting fluctuations (SF). (b) The Hall sign-reversal phase diagram. Shading shows Hall resistance $R_{xy}(B, T)$ for a 2 UC device with $T_c = 81.5$ K. The blue region shows the area of negative Hall resistance. Symbols show the locus $R_{xy} = 0$ for different thicknesses, and the lines are generated from fits to $R_{xy} = 0$ using Eq. (2) [13] (solid) and using Eq. (3) (dash). As thickness decreases, the Hall sign-reversed region becomes larger.

functional can be expressed in terms of collective variables representing topological vortex excitations. As observed in [2], it is the change from normal carrier- to the flux flow-dominated transport that causes the sign reversal in Hall resistance. Since the sign reversal is observed above T_c, one expects that the expansion of the TDGL with respect to vortex topological excitations will provide an adequate description of the Hall effect at temperatures from $T \gtrsim T_c$ down to zero. This program was realized in [13], where the Hall conductivity was derived as

$$\sigma_{xy} = \frac{\Delta^2 n_0 ec}{E_F^2 B}[(\tau\Delta/\hbar)^2 g - \mathrm{sgn}(\delta n)] + \sigma_{xy}^n(1-g). \quad (1)$$

Here, n_0 and n_∞ are the normal carrier density inside and outside the vortex core, respectively, and $\delta n = n_0 - n_\infty$ is the excess charge inside the vortex; τ is the relaxation time of the normal carrier in the vortex core; and parameter g expresses the SC fraction of the carriers. The second term in the rhs of Eq. (1) ensures a smooth transition to Hall conductivity dominated by normal carriers. We consider a two-fluid model of a d-wave symmetry superconductor [45] so that $g(T) = 1 - (T/T_c)^2$, where the value of T_c was previously determined from the analysis of $R_{xx}(B,T)$ with a SF description.

This result makes apparent that the physical origin of the Hall effect sign change is the excess charge δn of the vortex core, which is of the order of $n_0(\Delta/E_F)^2$ [13,43]. The sign of the vortex contribution is controlled by the relation between $\mathrm{sgn}(\delta n)$ and $\tau\Delta$. In the regime $T < T_c$, this empirically fixes $\mathrm{sgn}(\delta n) = 1$. Then, the first term in Eq. (1), the vortex core contribution σ_{xy}^{vc}, can be negative as $\Delta(T) < \hbar/\tau$. Furthermore, we note that $\sigma_{xy} \sim B^{-1}$ while $\sigma_{xy}^n \sim B$. Therefore, the total Hall sign reversal is expected at low magnetic fields, where negative vortex contribution σ_{xy}^{vc} dominates the positive normal carrier contribution σ_{xy}^n.

Using Eq. (1), we describe the phase boundary of the Hall sign-reversed region in Fig. 3(b) for all the samples under study. The sign-reversal locus, $R_{xy}(T,B) = 0$, follows from Eq. (1) and is defined by the relation

$$B^2 = \left(\frac{\Delta}{E_F}\right)^2 \frac{n_0 c}{S_{xy}^n}\frac{[(\Delta\tau/\hbar)^2 g - 1]}{1-g}, \quad (2)$$

where we estimate the normal contribution σ_{xy}^n using the empirical observation $\sigma_{xy} = S_{xy}^n(T)B$ in the normal state far enough from T_c, where $S_{xy}^n(T) \propto T^{-2}$ (see Fig. 4 in the Supplemental Material [19]), we extrapolate this dependence to low temperatures. Then, we fit our data shown in Fig. 3(b) with Eq. (2), using as fitting parameters τ and n_0/E_F^2 (numerical values of all parameters are given in Table I in the Supplemental Material [19]). We obtain the relaxation rate of the normal carriers in the vortex core $\tau \approx 0.08$ ps. This agrees with the quasiparticle lifetime estimated from the scanning tunneling spectroscopy of the vortex cores in BSCCO [46] observing normal quasiparticle excitations at $E \approx 7$ meV, giving the crude estimate $\tau \approx \hbar/E \approx 0.1$ ps. The value $n_0/E_F^2 \approx (1-2)\times 10^{21}$ cm^{-3} eV^{-2} is in satisfactory agreement with the widely accepted value $n_0 \approx 10^{21}$ cm^{-3} in cuprates [47] and with the fact that E_F of cuprates is often an order of magnitude larger than the superconducting gap $\Delta(0)$ [48] which is $\Delta(0) \approx 0.02$ eV in our case. For the temperature dependence $\Delta(T)$, we take the temperature dependence of the d-wave gap [with $\Delta(0)/k_B T_{\mathrm{HSR}} = 2.15$] [49] where T_{HSR} is the upper temperature of the onset of the Hall sign reversal (see Table in Supplemental Material [19]). The d-wave description of $\Delta(T)$ is also supported by STM measurements on BiO terraces in BSCCO [50], although tunnel spectra of exposed CuO_2 terraces suggests a nodeless SC gap [50,51]. Temperature dependencies of superconducting gap $\Delta(T)/T_c$ vs T/T_c are shown in the inset of Fig. 3(a) for all samples. Note that T_{HSR} determined from our fits appeared to be higher than T_c, implying nonzero $\Delta(T_c)$, which is in agreement with experimental observations in tunneling [52] and in angle-resolved photoemission spectroscopy [53].

Equation (2) for the dome-shaped sign-reversal phase boundary correctly describes the sign-reversal enhancement as samples become thinner (Fig. 3). As the mobility μ_H decreases with thickness [Fig. 2(c)], σ_{xy}^n is suppressed in turn. Since μ_H is in the denominator in Eq. (2), the decrease of μ_H leads to enhancement of dome size. In other words, the contribution from topological excitation has more effect on the conductivity σ_{xy} when the normal component σ_{xy}^n decreases [see Eq. (1)].

The curve $R_{xy}(B,T) = 0$ defined by Eq. (2) demonstrates an excellent agreement with the experimental data shown in Fig. 3(b) both for $T < T_c$ and for $T > T_c$. Using the same fitting parameters we compare the whole R_{xy} evolution with the vortex expansion of the TDGL. Figures 2(a) and 3(a) show the fits of R_{xy} at fixed T and B, respectively, in dashed lines, calculated according to Eq. (1) using $\rho_{xy} = \sigma_{xy}\rho_{xx}^2$. The vortex dynamics description agrees well with the experiment in a wide region in temperature $T < T_c$ and magnetic field. For $T > T_c$ the agreement is still fair; however, we observe some deviation of theoretical curve from experimental R_{xy} [see curve at 80 K in Fig. 2(a)], the deviation growing with increasing temperature [54].

To cross-check the applicability of the vortex-based description of $R_{xy}(B)$ and $R_{xy}(T)$ at $T > T_c$, we employ the superconducting fluctuation expansion of TDGL, using the smallness of the order parameter in the fluctuation regime. Qualitatively, SF are Cooper pairs with a finite lifetime, arising above T_c. Under applied magnetic field, these pairs rotate around their center of mass and can be viewed as elemental current loops. The external current exerts Magnus force moving these loops along the circular paths. This gives rise to Hall voltage opposite to that from the normal carriers. The SF contribution to Hall conductivity manifests as a negative correction $\delta\sigma_{xy}$ to the positive normal component σ_{xy}^n [10,32]: $\sigma_{xy} = \sigma_{xy}^n + \delta\sigma_{xy}$. Expression for $\delta\sigma_{xy}$ in the Gaussian approximation [10] is

$$\delta\sigma_{xy} = \frac{2e^2 k_B T}{hd}\zeta f(D,B,T), \quad (3)$$

where D is the normal carrier diffusion coefficient evaluated as $D \approx \frac{2}{3}\mu_H E_F$ (see Supplemental Material [19] Sec. E); f is a dimensionless function (see Supplemental Material [19] for explicit form); ζ is a parameter accounting for particle-hole asymmetry in the time-dependent Ginzburg-Landau equation. The parameter ζ is expressed as the change of T_c with respect to the chemical potential μ: $\zeta = -\frac{1}{2}\partial(\ln T_c)/\partial\mu \approx 1/(\gamma E_F)$ [10,32,55]. Here, γ is the dimensionless coupling constant parametrizing the attractive electron-electron interaction that induces superconductivity. As temperature decreases, the SF contribution $\delta\sigma_{xy}$ increases, leading to the sign change of σ_{xy} as soon as $\delta\sigma_{xy}$ starts to dominate [41,42,56]. The Hall resistance $R_{xy}(B)$ and $R_{xy}(T)$ at $T > T_c$ is nicely described by the SF description of Eq. (3) [dash-dotted line in Figs. 2(a) and 3(a)], where the values of fitting parameter γE_F (see Supplemental Material [19]) correspond to $\gamma < 1$ (the weak coupling limit) and E_F previously evaluated from fits of $R_{xy}(B,T) = 0$ with Eq. (2). The phase boundary for $T > T_c$ is also accurately captured by the SF description in Eq. (3) [Fig. 3(b), dashed line]. Remarkably, for $T > T_c$, the phase boundary $R_{xy}(T,B) = 0$ agrees with both vortex and SF TDGL asymptotes. The agreement between the values of E_F and fits of the phase boundary provides a cross-check ensuring that vortex description of Eq. (2) works fairly well at $T > T_c$. Thus, our findings support the idea that vortexlike excitations survive above T_c [57] in full concert with Nernst effect observations [14,15]. Our results apply to any bulk HTS with layered structure. Also, since disorder enters through the scattering time, our conclusions remain valid for disordered low-T_c films; see, e.g., [58,59].

In conclusion, we developed van der Waals assembly techniques specialized to the cuprates. We fabricated few-unit-cell $Bi_{2.1}Sr_{1.9}CaCu_{2.0}O_{8+\delta}$ crystals, where an appreciable enhancement of the Hall sign reversal with the system's thinning was observed. We demonstrated that the Hall resistance sign reversal occurs both below and above T_c and is well described in terms of vortex dynamics across the entire temperature interval. In the fluctuation region above T_c, the sign reversal is equally well described by superconducting fluctuation formalism which cross-checks our results and connects vortexlike excitations above T_c and superconducting fluctuations.

The experiments were supported by NSF (DMR-1809188) and the Moore Foundation EPiQS Initiative (GBMF4543). Stencil masks were fabricated at Harvard CNS, a part of National Nanotechnology Coordinated Infrastructure, NSF 1541959. S. Y. F. Z. and N. P. were partially supported by NSERC PGS and ARO (W911NF-17-1-0574). G. D. G., R. Z., V. M. V. are supported by the U.S. Department of Energy under Contract No. de-sc0012704, Center for Emergent Superconductivity (an Energy Frontier Research Center), and Basic Energy Sciences (Materials Sciences and Engineering Division), respectively. S. V. P. is supported by the Russian Science Foundation, Grant No. 15-12-10020.

*Corresponding author.
pkim@physics.harvard.edu

[1] Y. Cao, V. Fatemi, S. Fang, K. Watanabe, T. Taniguchi, E. Kaxiras, and P. Jarillo-Herrero, Nature (London) **556**, 43 (2018).
[2] M. P. A. Fisher, Physica (Amsterdam) **177A**, 553 (1991).
[3] A. T. Dorsey and M. P. A. Fisher, Phys. Rev. Lett. **68**, 694 (1992).
[4] Z. D. Wang, J. M. Dong, and C. S. Ting, Phys. Rev. Lett. **72**, 3875 (1994).
[5] N. B. Kopnin, Phys. Rev. B **54**, 9475 (1996).
[6] Y. Kato, J. Phys. Soc. Jpn. **68**, 3798 (1999).
[7] J. Koláček and P. Vašek, Physica (Amsterdam) **336C**, 199 (2000).
[8] S. Ullah and A. T.Dorsey, Phys. Rev. B **44**, 262 (1991).
[9] T. Nishio and H. Ebisawa, Physica (Amsterdam) **290C**, 43 (1997).
[10] K. Michaeli, K. S. Tikhonov, and A. M. Finkelstein, Phys. Rev. B **86**, 014515 (2012).
[11] P. Ao and D. J. Thouless, Phys. Rev. Lett. **70**, 2158 (1993).
[12] D. I. Khomskii and A. Freimuth, Phys. Rev. Lett. **75**, 1384 (1995).
[13] M. V. Feigelman, V. B. Geshkenbein, A. I. Larkin, and V. M. Vinokur, JETP Lett. **62**, 834 (1995).
[14] Z. A. Xu, N. P. Ong, Y. Wang, T. Kakeshita, and S. Uchida, Nature (London) **406**, 486 (2000).
[15] Y. Wang, Z. A. Xu, T. Kakeshita, S. Uchida, S. Ono, Y. Ando, and N. P. Ong, Phys. Rev. B **64**, 224519 (2001).
[16] L. J. Sandilands, A. A. Reijnders, A. H. Su, V. Baydina, Z. Xu, A. Yang, G. Gu, T. Pedersen, F. Borondics, and K. S. Burch, Phys. Rev. B **90**, 081402(R) (2014).
[17] R. P. Vasquez, J. Electron Spectrosc. Relat. Phenom. **66**, 209 (1994).
[18] N. Poccia, M. Fratini, A. Ricci, G. Campi, L. Barba, A. Vittorini-Orgeas, G. Bianconi, G. Aeppli, and A. Bianconi, Nat. Mater. **10**, 733 (2011).
[19] See Supplemental Material at http://link.aps.org/supplemental/10.1103/PhysRevLett.122.247001 for detailed methods, SF analysis of $R_{xx}(T)$, Hall sign reversal in 3 UC device, Hall fitting using SF approximation, and magnetoresistance data, which includes Refs. [17,20–29].
[20] M. Fratini, N. Poccia, A. Ricci, G. Campi, M. Burghammer, G. Aeppli, and A. Bianconi, Nature (London) **466**, 841 (2010).
[21] L. Wang *et al.*, Science **342**, 614 (2013).
[22] R. I. Razouk and A. S. Salem, J. Phys. Chem. **52**, 1208 (1948).
[23] A. Castellanos-Gomez, M. Buscema, R. Molenaar, V. Singh, L. Janssen, H. S. J. van der Zant, and G. A Steele, 2D Mater. **1**, 011002 (2014).

[24] A. Bianconi, M. Lusignoli, N. L. Saini, P. Bordet, A. Kvick, and P. G. Radaelli, Phys. Rev. B **54**, 4310 (1996).

[25] G. Balestrino, E. Milani, C. Aruta, and A. A. Varlamov, Phys. Rev. B **54**, 3628 (1996).

[26] J. M. B. L. dos Santos and E. Abrahams, Phys. Rev. B **31**, 172 (1985).

[27] T. I. Baturina, S. V. Postolova, A. Yu. Mironov, A. Glatz, M. R. Baklanov, and V. M. Vinokur, Europhys. Lett. **97**, 17012 (2012).

[28] P. Minnhagen, Phys. Rev. B **23**, 5745 (1981).

[29] P. Minnhagen, Rev. Mod. Phys. **59**, 1001 (1987).

[30] *High-Temperature Superconductors*, edited by X. G. Qiu (Woodhead Publishing, Ltd., Cambridge, 2011).

[31] J. S. Wen, Z. J. Xu, G. Y. Xu, M. Hucker, J. M. Tranquada, and G. D. Gu, J. Cryst. Growth **310**, 1401 (2008).

[32] A. I. Larkin and A. A. Varlamov, *Theory of Fluctuations in Superconductors* (Oxford University Press, New York, 2005).

[33] S. V. Postolova, A. Y. Mironov, M. R. Baklanov, V. M. Vinokur, and T. I. Baturina, Sci. Rep. **7**, 1718 (2017).

[34] M. Truccato, A. Agostino, G. Rinaudo, S. Cagliero, and M. Panetta, J. Phys. Condens. Matter **18**, 8295 (2006).

[35] S. V. Postolova, A. Yu. Mironov, and T. I. Baturina, JETP Lett. **100**, 635 (2015).

[36] B. L. Altshuler and A. G. Aronov, *Electron-Electron Interaction in Disordered Systems*, edited by A. L. Efros and M. Pollak (North-Holland, Amsterdam; Elsevier, New York, 1985).

[37] P. G. Baity, X. Shi, Z. Shi, L. Benfatto, and D. Popovic, Phys. Rev. B **93**, 024519 (2016).

[38] A. Pomar, M. V. Ramallo, J. Mosqueira, C. Torron, and F. Vidal, Phys. Rev. B **54**, 7470 (1996).

[39] C. Torron, A. Diaz, A. Pomar, J. A. Veira, and F. Vidal, Phys. Rev. B **49**, 13143 (1994).

[40] A. L. Solovev and V. M. Dmitriev, Low Temp. Phys. **35**, 169 (2009).

[41] N. P. Breznay, K. Michaeli, K. S. Tikhonov, A. M. Finkelstein, M. Tendulkar, and A. Kapitulnik, Phys. Rev. B **86**, 014514 (2012).

[42] D. Destraz, K. Ilin, M. Siegel, A. Schilling, and J. Chang, Phys. Rev. B **95**, 224501 (2017).

[43] K. Nakao, K. Hayashi, T. Utagawa, Y. Enomoto, and N. Koshizuka, Phys. Rev. B **57**, 8662 (1998).

[44] W. Liu, T. W. Clinton, A. W. Smith, and C. J. Lobb, Phys. Rev. B **55**, 11 (1997).

[45] M. Tinkham, *Introduction to Superconductivity*, 2nd ed. (McGraw-Hill, New York, 1996).

[46] S. H. Pan, E. W. Hudson, A. K. Gupta, K.-W. Ng, H. Eisaki, S. Uchida, and J. C. Davis, Phys. Rev. Lett. **85**, 1536 (2000).

[47] A. T. Bollinger and I. Božović, Supercond. Sci. Technol. **29**, 103001 (2016).

[48] A. K. Saxena, *High-Temperature Superconductors* (Springer, Berlin/Heidelberg, 2012).

[49] H. Won and K. Maki, Phys. Rev. B **49**, 1397 (1994).

[50] S. Misra, S. Oh, D. J. Hornbaker, T. DiLuccio, J. N. Eckstein, and A. Yazdani, Phys. Rev. Lett. **89**, 087002 (2002).

[51] Y. Zhong *et al.*, Sci. Bull. **61**, 1239 (2016).

[52] J. K. Ren, X. B. Zhu, H. F. Yu, Y. Tian, H. F. Yang, C. Z. Gu, N. L. Wang, Y. F. Ren, and S. P. Zhao, Sci. Rep. **2**, 248 (2012).

[53] M. Hashimoto, I. M. Vishik, R. H. He, T. P. Devereaux, and Z. X. Shen, Nat. Phys. **10**, 483 (2014).

[54] The reason for that is that the dome configuration is determined solely by the condition $\sigma_{xy} = 0$ and the behavior ρ_{xx} is irrelevant. At the same time, the behavior of ρ_{xy} accounts for the finite residual resistance ρ_{xx} at $B = 0$, which is omitted in the vortex approximation [2].

[55] A. A. Varlamov, G. Balestrino, E. Milani, and D. V. Livanov, Adv. Phys. **48**, 655 (1999).

[56] K. Makise, F. Ichikawa, T. Asano, and B. Shinozaki, J. Phys. Condens. Matter **30**, 065402 (2018).

[57] A. Glatz, A. A. Varlamov, and V. M. Vinokur, Europhys. Lett. **94**, 47005 (2011).

[58] A. Yu. Mironov, S. V. Postolova, and T. I. Baturina, J. Phys. Condens. Matter **30**, 485601 (2018).

[59] M. V. Burdastyh, S. V. Postolova, T. I. Baturina, T. Proslier, V. M. Vinokur, and A. Yu. Mironov, JETP Lett. **106**, 749 (2017).